Field curvature correction method for ultrashort throw ratio projection optics design using an odd polynomial mirror surface

Zhenfeng Zhuang,[1] Yanting Chen,[2] Feihong Yu,[2,*] and Xiaowei Sun[1]

[1]School of Electrical and Electronic Engineering, Nanyang Technological University, 50 Nanyang Avenue, Singapore 639798, Singapore

[2]Optical Engineering Department, Zhejiang University, Hangzhou 310027, China

*Corresponding author: feihong@zju.edu.cn

Received 24 February 2014; revised 19 July 2014; accepted 21 July 2014; posted 22 July 2014 (Doc. ID 206555); published 1 August 2014

This paper presents a field curvature correction method of designing an ultrashort throw ratio (TR) projection lens for an imaging system. The projection lens is composed of several refractive optical elements and an odd polynomial mirror surface. A curved image is formed in a direction away from the odd polynomial mirror surface by the refractive optical elements from the image formed on the digital micromirror device (DMD) panel, and the curved image formed is its virtual image. Then the odd polynomial mirror surface enlarges the curved image and a plane image is formed on the screen. Based on the relationship between the chief ray from the exit pupil of each field of view (FOV) and the corresponding predescribed position on the screen, the initial profile of the freeform mirror surface is calculated by using segments of the hyperbolic according to the laws of reflection. For further optimization, the value of the high-order odd polynomial surface is used to express the freeform mirror surface through a least-squares fitting method. As an example, an ultrashort TR projection lens that realizes projection onto a large 50 in. screen at a distance of only 510 mm is presented. The optical performance for the designed projection lens is analyzed by ray tracing method. Results show that an ultrashort TR projection lens modulation transfer function of over 60% at 0.5 cycles/mm for all optimization fields is achievable with f-number of 2.0, 126° full FOV, <1% distortion, and 0.46 TR. Moreover, in comparing the proposed projection lens' optical specifications to that of traditional projection lenses, aspheric mirror projection lenses, and conventional short TR projection lenses, results indicate that this projection lens has the advantages of ultrashort TR, low f-number, wide full FOV, and small distortion.

OCIS codes: (120.4570) Optical design of instruments; (220.4830) Systems design; (080.4225) Nonspherical lens design.

http://dx.doi.org/10.1364/AO.53.000E69

1. Introduction

Compared with traditional cathode ray tube (CRT) projectors, digital micromirror device (DMD) projectors based on light-emitting diodes (LEDs) have many advantages, such as brightness, resolution, and compact size [1–3]. With the gradually increasing application in the fields of business, education, household, and digital cinema, digital light processing (DLP) projectors have advanced rapidly in recent years due to a fast-growing consumer market. For these applications, a large screen projected at an ultrashort distance is demanded by consumers. Using a conventional projector, the shadow of the presenter or teacher may appear on the screen and the glare of

1559-128X/14/220E69-08$15.00/0

the projected light will hit the presenter's eyes. Moreover, a lot of space is wasted. The entire table needs to be clear or the image is partially obscured. For the current DLP projection optical engine, multiple glass optical elements are generally used to achieve higher optical performance, so as to shorten the projection distance while keeping a large projection size. This inevitably leads to an increased lens diameter because of the wide field of view (FOV). A fisheye lens, which is a wide-angle lens that projects a wide image, can be used; however distortion is inevitable when we use a fisheye lens with a wide FOV and a low f-number. There has been great demand for the design of an optical system that can project onto a large screen at an ultrashort distance with low distortion and small f-number.

Many remarkable projection display systems have proposed in several patents by the NEC designer Ogawa [4], Hitachi designers Hirata *et al.* [5], and Inovel designer Lu [6] to achieve an extraordinarily large projection angle with low distortion. The reflecting mirror surface used in these can be concave or convex, and the projected screen may achieve a size from 50 to 80 in. diagonal. The distance between the projector and the screen is less than 1 m. None of them mention the design method of their work in detail.

A freeform mirror surface provides larger degrees of freedom to design an optical surface, and methods such as the partial differential equation [7,8] and simultaneous multiple surfaces (SMS) [9,10] can be used. Freeform optics is always used to achieve a projection lens system that fulfills the above-mentioned requirements. Based on the linear relationship between the angle of incidence of light onto a surface and the angle of reflection onto the imaging device, Hicks [11] derived a differential equation and generated surface shapes. However, this method is not suitable for cameras with relatively large apertures, as the chief ray of each FOV is used to calculate the aspheric mirror profile. For the design of a compact structure, four-mirror aspheric-type projector [12–14] was being designed as a projector. However, the problem of tilt or decenter of the mirror surface makes it difficult for optical designers to fix them. In recent years, Miñano and co-workers [15–18] have applied the SMS method to designing the imaging optics. An extremely large image was obtained using two mirrors combined with a conventional projector. However, they also did not put forward the detailed design method in their paper.

In this paper, we propose a field curvature correction (FCC) method to achieve an extraordinary screen size at an ultrashort distance with low distortion, small f-number, and an extraordinarily large projection angle by using an odd polynomial mirror surface combined with a set of refractive optical elements. A curved image that is formed by these elements and the desired large screen with low distortion is magnified by an odd polynomial mirror surface according to the FCC approach. The laws of reflection determine the chief ray from the exit pupil of each FOV from the corresponding predescribed position on the screen, and a freeform mirror surface is calculated with segments of hyperbolic from the differential equation as an initial design profile. The value of the high-order odd polynomial surface is then used to express of the freeform mirror surface. Using this method, an ultrashort TR projection lens with low distortion can be obtained.

The rest of the paper is organized as follows. In Section 2, the FCC approach is introduced, and we also describe the method of designing the initial freeform mirror surface by using hyperbolic segments. In Section 3, a design example is described and its optical performance is analyzed. Finally, the conclusions are drawn in Section 4.

2. Design Methodology

A. FCC Method

Figure 1 shows the design principle of this method of correcting field curvature that is generated by the convex mirror surface. OB and IM are employed to denote, respectively, the object and the image. As shown in Fig. 1(a), OB is an erect, virtual object with respect to the mirror surface and IM is an image of the OB formed by the mirror surface. It is shown that a curvature of field is produced by the convex mirror surface. The IM of plane object OB is curved as image height increases. As shown in Fig. 1(b), OB is the curved, virtual object with respect to the freeform mirror surface and IM is an erect, real image. A virtual object is curved in advance in a direction away from the convex mirror. The field curvature produced by the virtual object is considered to be canceled by the mirror surface and an erect image can be obtained. In this case, the image formed by the mirror surface is erect, real, and is magnified. So, the key to this method is designing a convex mirror surface that can correct field curvature and form a plane image on the screen.

B. Design of the Odd Polynomial Mirror Surface

Figure 2 is a diagram illustrating the layout of the projection system, which is composed of several refractive optical elements and a convex mirror surface arranged along the common optical axis (OA). In Fig. 2, a curved virtual image is formed from the image on the DMD panel. The curved virtual image is curved in advance in a direction away from the convex mirror surface as the DMD panel height increases. The convex mirror surface cancels the field curvature and an enlarged plane image with no curve can be displayed on the screen.

The difficulty of this projection system, which includes a convex odd polynomial mirror surface, lies in the simultaneous design of refractive lenses and reflective mirror surfaces. As in every imaging system, the optical system is described by its entrance and exit pupils. It is difficult to match exit pupil distance and chief ray angle by the reverse design

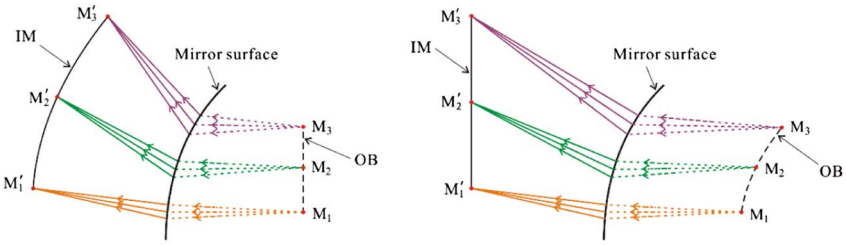

Fig. 1. Schematic illustration of the FCC method. (a) Field curvature caused by the convex mirror surface. A curved and enlarged image of an erect object by the convex mirror surface is obtained. (b) Approach of correcting the field curvature caused by the concave mirror surface. A plane and enlarged image of a curved object by the convex mirror surface is obtained.

approach, so this was given up after several failed attempts. After several trials the forward-design method was chosen.

Since forward-design methodology is applied here, only the exit pupil is considered in the computation of the emergent rays from the exit pupil of each FOV, as shown in Fig. 3. The center of the exit pupil is set as the origin of the Cartesian coordinate system, and a z axis along the OA is established. The emergent rays coming from the same FOV are converged in a direction away from the convex mirror surface. In Fig. 3, the curved virtual image consists of three fields of view: M_1, M_2, and M_2, which are reflected by the convex surface and converge at points M'_1, M'_2, and M'_3 on the screen, respectively.

In contrast to conventional methods, freeform optics provides larger degrees of freedom to design an optical surface. This convex mirror surface could be established by hyperbolic segments [19–21]. An ordinary hyperbolic surface is one that brings light from the first focal point to another target point on the screen, i.e., points M_1 and M'_1 are the two foci of the reference hyperbolic segment.

For the first FOV, as shown in Fig. 4, we assume that **R** is the vector of the emergent ray at point M_1, and it passes through the center of the original exit pupil that all of the chief rays pass through. The polar radius ρ is the distance between origin point O and point M_1 of the intermediate imaging. From Fig. 4, the vector **R** can be expressed as

$$\mathbf{R}_{(\mathbf{m})} = \rho \times \mathbf{m}, \tag{1}$$

where **m** denotes the unit vector of the emergent ray, which is given by Eq. (2) in Cartesian coordinates:

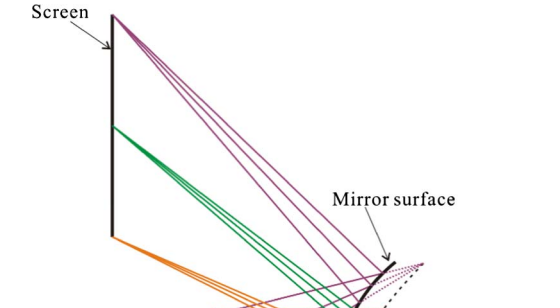

Fig. 2. Diagrammatic representation of the projection system that includes a convex mirror surface.

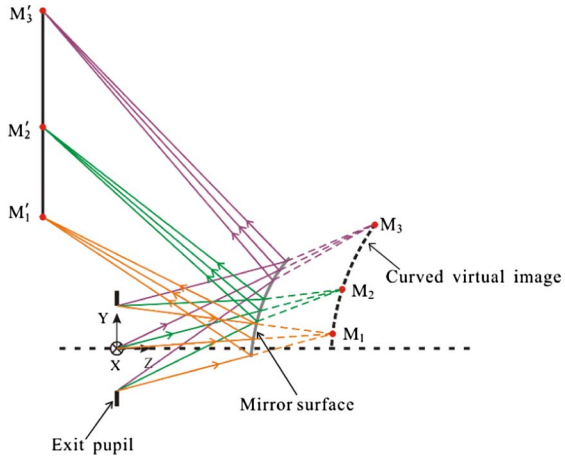

Fig. 3. Optical principle of the mirror surface.

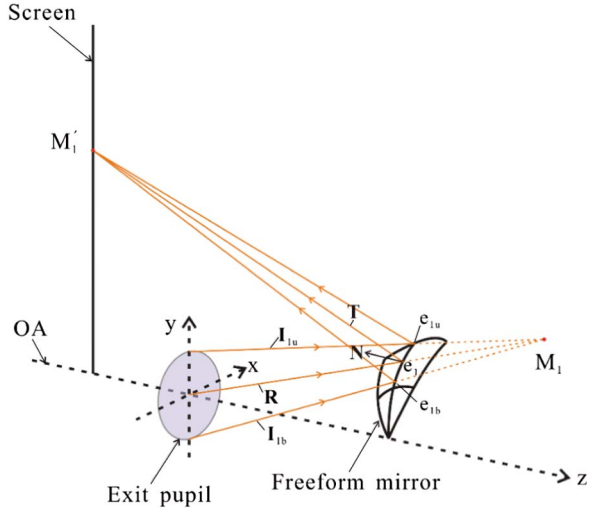

Fig. 4. Determination of the reference surface segment by hyperbolic segments.

$$\mathbf{m} = [\sin(\varphi) \times \cos(\theta), \sin(\varphi) \times \sin(\theta), \cos(\varphi)]. \quad (2)$$

Here, φ is the angle between the emergent ray and OA, θ is the angle between emergent ray projection on plane XOY and OA, and $\mathbf{T}$ is the vector of the reflective ray from the freeform mirror surface from point e_1 to point M_1'. According to the laws of reflection, the relationship between the unit vector $\mathbf{m}$ of the emergent ray and the unit vector $\mathbf{T}$ of the reflected ray at point e_1 can be written as [22,23]

$$\mathbf{T} = \mathbf{m} - 2 \times (\mathbf{m} \times \mathbf{N}) \times \mathbf{N}, \quad (3)$$

where $\mathbf{N}$ is the unit normal of the freeform mirror surface at point e_1.

As mentioned above, this method uses the reflective property of hyperbolic segments to establish the reflector surface. In a polar coordinate system, the profile of the hyperbolic surface can be expressed as [21]

$$\rho_{(\mathbf{m})} = \frac{d}{\kappa(\mathbf{m} \times \hat{\mathbf{v}}) - 1}, \quad (4)$$

where d is the focal parameter, $\mathbf{v}$ is the vector directing to another focal point of the hyperbolic segment of revolution, and $\kappa(\kappa > 1)$ is the eccentricity, which can be calculated from the basic properties of hyperbolic segments as

$$\kappa = \sqrt{1 + \frac{d^2}{|\mathbf{v}|^2}} - \frac{d}{|\mathbf{v}|}. \quad (5)$$

If we know the initial focal parameter of the reference hyperbolic segment, by using Eqs. (1)–(5), we can get the radius vector $\mathbf{R}$ of the freeform mirror surface. For a rotationally symmetric optical system, the other two reference rays of each FOV from the exit pupil are defined, such as the upper meridional ray and the bottom meridional ray; $\mathbf{I_{1u}}$ and $\mathbf{I_{1b}}$ are incident rays of the upper marginal ray and the bottom marginal ray, respectively. The two edge points of the convex mirror surface, e_{1u} and e_{1b}, are the points of the intersection of rays $\mathbf{I_{1u}}$ and $\mathbf{I_{1b}}$ with the reference hyperbolic segment, which can be calculated by the bisection method [24].

For the second FOV, we place one focus of the hyperbolic segment at point M_2 and the other focus at given target screen point location M_2', as shown in Fig. 5. Other segments of the hyperbolic should be larger than the reference hyperbolic segment, and a constraint of all focal parameters must be satisfied as shown in Eq. (6):

$$d_k > d_1, \qquad (k = 1, \ldots, P-1, P), \quad (6)$$

where k is the kth FOV, and P denotes the whole FOV. The bisection method is used to compute the other focal parameter d_k of a hyperbolic segment until the second hyperbolic segment satisfies the continuity condition:

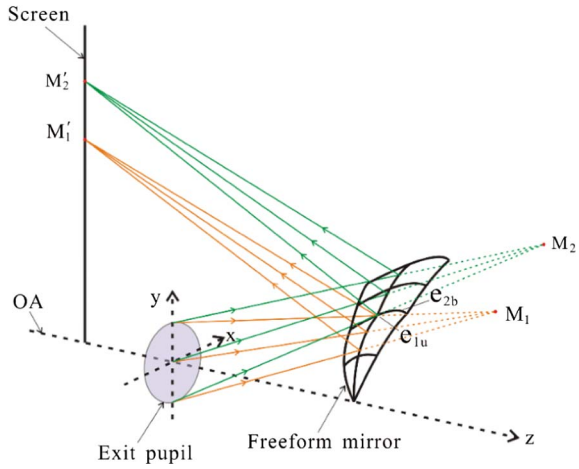

Fig. 5. Determination of the second hyperbolic surface segment.

$$e_{1u} = e_{2b}, \quad (7)$$

where e_{1u} denotes the intersection point of the upper meridional ray with the reference hyperbolic segment, and e_{2b} represents the intersection point of the bottom meridional ray with the second hyperbolic segment. Then, the same procedure is repeated for each of the remaining FOVs of the imaging system. The entire convex mirror surface is assembled by hyperbolic segments. Thus, it can be written as [25]

$$R_{\text{mirror surface}} = \bigcup_{k=1}^{P} A_k, \quad (8)$$

where $R_{\text{mirror surface}}$ is the area of the mirror surface, and A_k is the region of the kth hyperbolic segment.

Finally, the convex mirror surface $R_{\text{mirror surface}}$ is fitted using the odd polynomial surface, aiming to analyze the optical performance of the projection optics. The expression of odd polynomial surface is

$$z = \frac{c \times r^2}{1 + \sqrt{1 - (1 + k) \times c^2 \times r^2}} + A_1 \times r + A_2 \times r^2 + \cdots + A_{30} \times r^{30}, \quad (9)$$

where z is sag; k is the conic constant; c is the curvature of the reflective surface; $r = \sqrt{x^2 + y^2}$ is the height above the OA; and $A_1, A_2, \ldots, A_{30}$ are

Table 1. Optical Specifications of the Ultrashort TR Projector System

Parameters	Specifications
Active area of DMD (mm^2)	9.85 × 6.16
Wavelength (nm)	430–650
Effective focus length (mm)	−4.6
Entrance pupil position (mm)	>200
f-number	2.0
Projection distance (mm)	510
Screen size (in.)	50

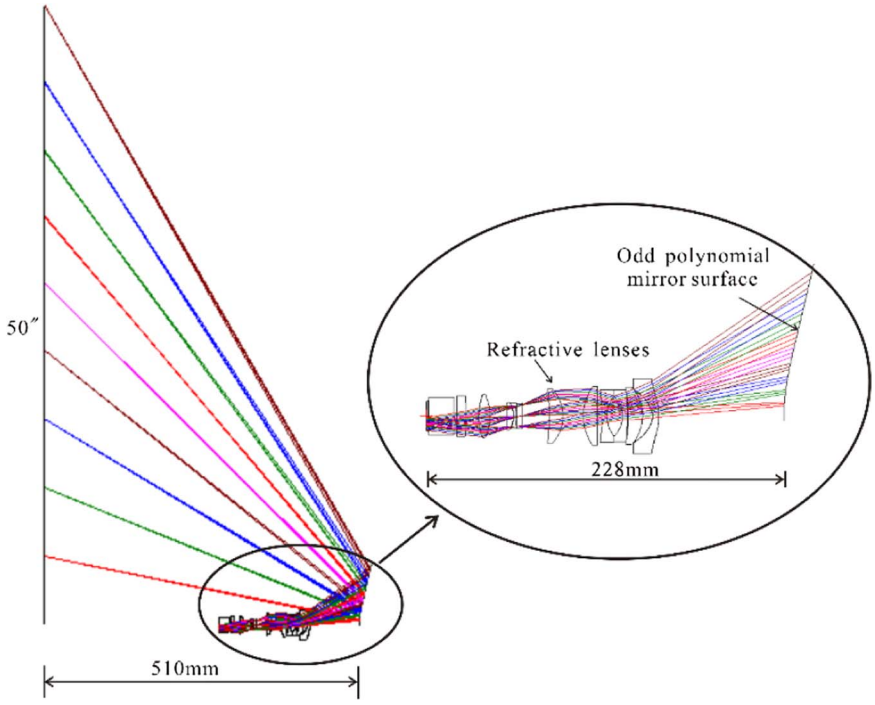

Fig. 6. Layout of the ultrashort TR projection system.

coefficients of the odd polynomial equation. The coefficients are used to correct for distortion.

Based on the above design methods, we obtained the initial projection system, which had considerable aberrations and distortion. A damped-least-squares optimization method is used to meet the design requirements.

3. Design Example and Analysis

In this section, an example is presented to verify the design method, and a ray-tracing simulation approach in imaging design software is applied to analyze the optical performance of the proposed projection system.

A. Layout and Specifications

The design optical specifications of the optical system are listed in Table 1, and the corresponding layout of the designed projection system is illustrated in Fig. 6. The projection system is a telecentric system in object space. The projection lens consists of eleven refractive optical elements and an odd polynomial convex mirror surface. The total track of the designed projection system, including the odd polynomial mirror surface, is about 228 mm, which demonstrates the unique behavior of the compact structure. The distance between the projector and the screen is only 510 mm. A diagonal 0.45 in. (11.43 mm) DMD with 1280 × 800 pixels and a 7.5 μm pixel size is chosen as the image panel.

B. Analysis and Comparisons

1. *Analysis of the Convex Mirror Surface*

The design result of the odd polynomial convex mirror surface is now considered. The initial and final profiles of the odd polynomial mirror surfaces are compared in Fig. 8. A set of discrete data points can be obtained by the approach described in Section 2, and the starting profile is constructed by fitting these points with an odd polynomial surface. The final optimization surface is plotted in Fig. 7 in red. The size of the optimized odd polynomial mirror surface is larger than the initial surface. The three-dimensional profile of the surface is shown in Fig. 8(a) and the corresponding contour map of the profile is shown in Fig. 8(b). The surface is symmetrical about the x axis. Figure 9 shows a three-dimensional representation of the surface. The overall dimensions of this surface are about 98 mm length × 49.2 mm width × 24.6 mm height, which can be fabricated directly on an aluminum block surface by using the diamond

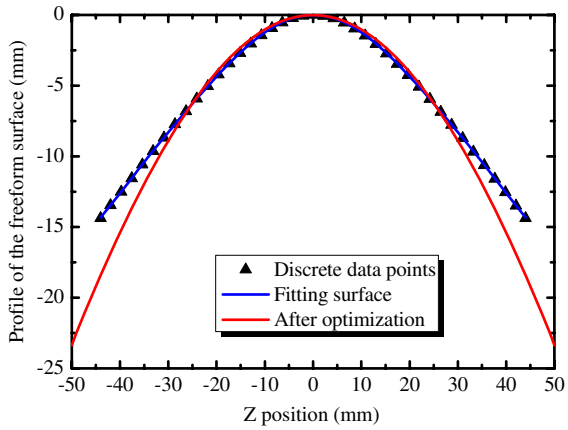

Fig. 7. Comparison of the shapes of the odd polynomial mirror surface before and after the optimization process.

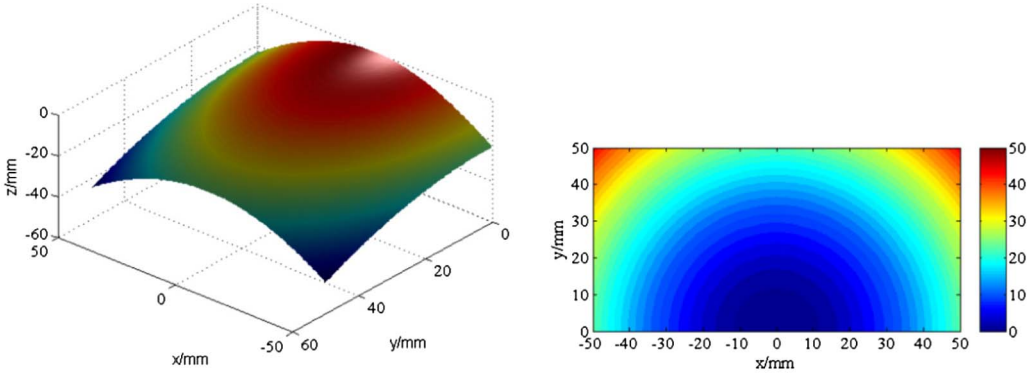

(a) (b)

Fig. 8. (a) Designed odd polynomial mirror surface profile. (b) Corresponding contour map of the odd polynomial mirror surface.

turning process. The surface is coated with a high-reflectance coating (over 99% reflection) during processing, which has been validated to achieve high luminous efficiency. The figure indicates that the surface shape is easily fabricated.

2. *Modulation Transfer Function*

The modulation transfer function (MTF) diagram of the ultrashort TR projection system is shown in Fig. 10, aiming to quantitatively evaluate the spatial resolution of the projection lens. The MTF shifts slightly with different wavelengths and field angles. In the image space, the cutoff frequency can be calculated as follows:

$$f_{\text{cutoff}} = \frac{1}{\eta} \times \frac{1000}{2 \times a}, \tag{10}$$

where a is the DMD's pixel size, and η is the projection magnification power. The spatial frequency is about 0.5 cycles/mm according to Eq. (10). The MTF value of a full field is above 60% at 0.5 cycles/mm for all optimization fields. It can be seen that almost all of the field is close to the diffraction limit.

3. *Distortion*

To evaluate the distortion of the designed projection lens, we can look at the image distortion grid of the projection. In [1], an approach for calculating the distortion of the image is proposed according to Eq. (11).

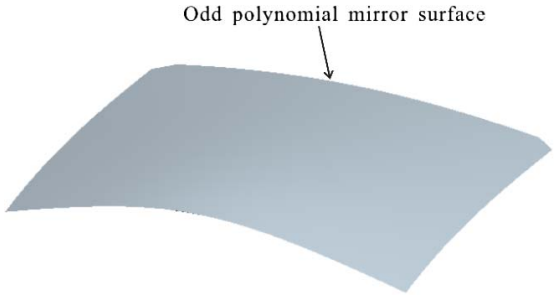

Fig. 9. Model of the odd polynomial mirror surface (overall dimensions: 98 mm × 49.2 mm × 24.6 mm).

When the distortion is lower than 1.5%, the image distortion cannot be observed by the human eye, so the image distortion of the projectors must be less than 1.5%. In Eq. (11), $H_{\min}$ is the minimal real image height, and H_l and H_r, respectively, are the left and right image heights without distortion:

$$\text{Dist} = \frac{0.5 \times (H_l + H_r) - H_{\min}}{H_{\min}} \times 100\%. \tag{11}$$

The distortion grid map of the projector is shown in Fig. 11. The maximum distortion is less than 1% at the bottom right and bottom left of the field according to Eq. (11).

4. *Throw Ratio*

One useful specification relating to the projector lens is its TR, which is defined as

$$\text{TR} = \frac{D}{W}, \tag{12}$$

where D is the distance between the projector lens and the projection screen and W is the width of

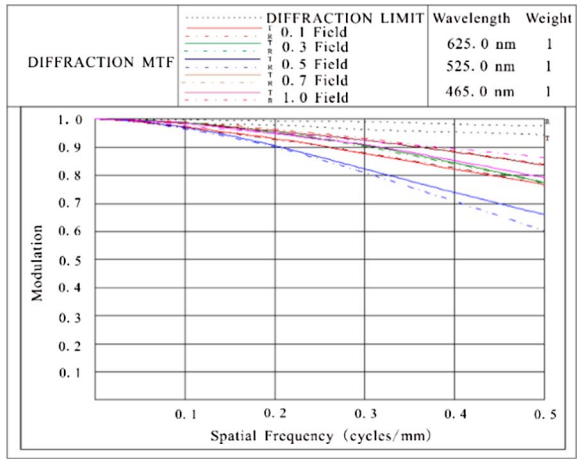

Fig. 10. MTF diagram in the image space. Different colors represent the tangential and sagittal MTFs of different fields. The black curve represents the MTF of diffraction limited data.

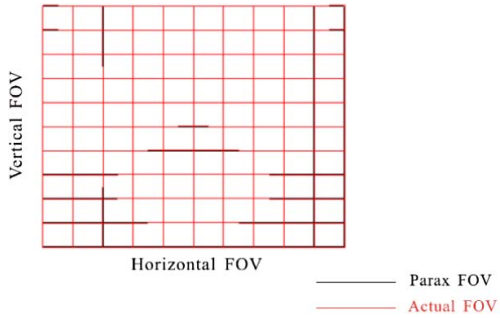

Fig. 11. Distortion grid map.

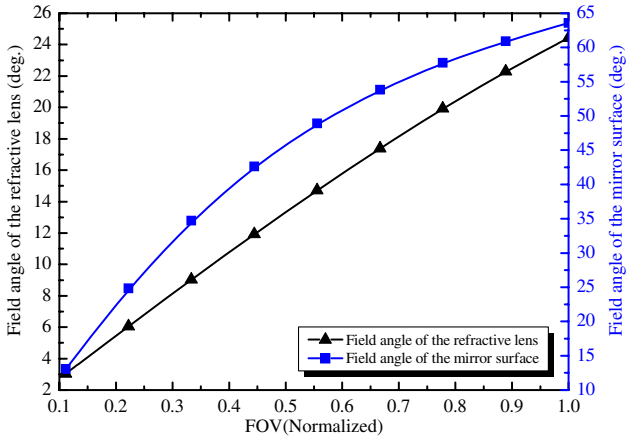

Fig. 12. Field angle of the refractive lens and field angle of the odd polynomial mirror surface versus normalized FOV.

the image being projected. A small value represents a larger screen of the same projection distance. The aspect ratio (AR) of the projector screen is 16:9, and the projector's TR is about 0.46, according to Eq. (12). Undoubtedly, an ultrashort TR projection system is obtained as the TR is less than 0.6.

5. *Full Field of View*

The relationship between field angle of the refractive optical elements, the field angle of the odd polynomial mirror surface, and normalized FOV is shown in Fig. 12. The field angle of the refractive optical elements increases linearly when the normalized FOV increases. The field angle of the odd polynomial mirror surface increases when the normalized FOV increases. In Fig. 12, the maximal FOV of the odd polynomial mirror surface is nearly 63°; thus, the full FOV is about 126°.

6. *Comparisons*

Our design of ultrashort TR projection system optical specifications is compared to those of the traditional projection lens [1], the aspheric-mirror projection lens [13], and the conventional short TR projection lens [6]; the results are listed in Table 2. We can obtain a lower TR, low f-number, and wider full FOV than the other designs. In our design, the projection lens is composed of several refractive lenses and a convex freeform mirror surface. This hybrid refractive–reflective (HRX) projection lens has many advantages. There is only one reflective surface, which makes it easy for optical designers to fix it, and it can be fabricated directly on an aluminum block surface by using the diamond turning process. In contrast to aspheric mirror projection lenses, the refractive lens is easier to manufacture. The manufacturing costs of aspheric mirror surfaces are high due to the complex procedures. Therefore, the designed projection lens could be easily fabricated at an extremely low cost. As a result, the designed HRX projection lens has outstanding optical performance and low cost.

4. Conclusions

In this paper, a new method for designing an ultrashort TR projection lens based on the FCC method is presented. This ultrashort TR projection lens is composed of refractive optical elements and an odd polynomial convex mirror surface. A curved virtual image is formed by the refractive optical elements from the image on the DMD panel, and then enlarged on the screen by the odd polynomial mirror surface. Based on the relationship between the chief ray from the exit pupil of each FOV and the corresponding predescribed position on the screen, the initial profile of the convex freeform mirror surface is calculated according to the laws of reflection by using hyperbolic segments. In addition, the freeform mirror surface could be fitted using the odd polynomial surface. Finally, an ultrashort TR projection lens is designed using

Table 2. Optical Specification Comparisons among Traditional Projection Lens, Aspheric-Mirror Projection Lens, Conventional Short TR Projection Lens, and Our Designed Projection Lens

	Traditional Projection Lens	Aspheric-Mirror Projection Lens	Conventional Short TR Projection Lens	Our Designed Projection Lens
Design type	Refractive only	Reflective only	HRX	HRX
Entrance pupil	Telecentric	Nontelecentric	Telecentric	Telecentric
f-number	2.4	2.5	2.8	2
Effective focal lengths	18.15 mm	—	−4.5 mm	−4.6 mm
Full FOV	53.4°	120°	130°	126°
Distortion	0.01%	<2.2%	<1%	<1%
Screen size (AR)	20 in. (16:9)	23 in.	50 in. (4:3)	50 in. (16:9)
TR	1.3	0.42	0.55	0.46

this method. Results show that the designed projection lens has several advantages, such as low f-number, small distortion, and wide full FOV. It is demonstrated that the designed projector has considerable potential for development and application.

The method proposed in this paper can also be used to achieve 50–100 in. diagonal projection screens at ultrashort distances.

The authors would like to thank Dr. Phil Surman for discussion and advice.

References

1. J. W. Pan, S. H. Tu, C. M. Wang, and J. Y. Chang, "High efficiency pocket-size projector with a compact projection lens and a light emitting diode-based light source system," Appl. Opt. **47**, 3406–3414 (2008).
2. J. W. Pan and S. H. Lin, "Achromatic design in the illumination system for a mini projector with LED light source," Opt. Express **19**, 15750–15759 (2011).
3. J. W. Pan and H. H. Wang, "High contrast ratio prism design in a mini projector," Appl. Opt. **52**, 8347–8354 (2013).
4. J. Ogawa, "Reflection type image forming optical system and projector," U.S. patent 6,612,704 B2 (2 September, 2003).
5. K. Hirata, M. Yatsu, T. Hisada, and M. Ohki, "Projection display system including lens group and reflecting mirror," U.S. patent 8,313,199 B2 (20 November, 2012).
6. K. C. Lu, "Wide angle projection and application," China patent 102967923 A (13 March, 2013).
7. J. Hou, H. F. Li, Z. R. Zheng, and X. Liu, "Distortion correction for imaging on non-planar surface using freeform lens," Opt. Commun. **285**, 986–991 (2012).
8. J. Hou, H. F. Li, R. M. Wu, P. Liu, Z. R. Zheng, and X. Liu, "Method to design two aspheric surfaces for imaging system," Appl. Opt. **52**, 2294–2299 (2013).
9. P. Benítez, J. C. Miñano, J. Blen, R. Mohedano, J. Chaves, O. Dross, M. Hernández, J. L. Alvarez, and W. Falicoff, "SMS design method in 3D geometry: examples and applications," Proc. SPIE **5185**, 18–29 (2004).
10. F. Muñoz, P. Benítez, O. Dross, J. C. Miñano, and B. Paikyn, "Simultaneous multiple surface design of compact air-gap collimators for light-emitting diodes," Opt. Eng. **43**, 1522–1530 (2004).
11. R. A. Hicks and R. Bajcsy, "Catadioptric sensors that approximate wide angle perspective projections," in *Proceedings of IEEE Conference on Computer Vision and Pattern Recognition* (IEEE, 2000), Vol. **1**, pp. 545–551.
12. J. Ogawa, K. Agata, and M. Sakamoto, "Super-short focus front projector with aspheric mirror projection optical system," SID J. **13**, 111–116 (2005).
13. Z. R. Zheng, X. T. Sun, X. Liu, and P. F. Gu, "Design of reflective projection lens with Zernike polynomials surfaces," Displays **29**, 412–417 (2008).
14. Z. R. Zheng, "Design of off-axis reflective projection lens using spherical Fresnel surface," Optik **122**, 145–149 (2011).
15. J. C. Miñano, P. Benítez, L. Wang, J. Infante, F. Muñoz, and A. Santamaría, "An application of the SMS method for imaging designs," Opt. Express **17**, 24036–24044 (2009).
16. F. Duerr, P. Benítez, J. C. Miñano, Y. Meuret, and H. Thienpont, "Analytic design method for optimal imaging: coupling three ray sets using two free-form lens profiles," Opt. Express **20**, 5576–5585 (2012).
17. F. Muñoz, P. Benítez, and J. C. Miñano, "High-order aspherics: the SMS nonimaging design method applied to imaging optics," Proc. SPIE **7100**, 71000K (2008).
18. J. C. Miñano, P. Benítez, L. Wang, F. Muñoz, J. Infante, and A. Santamaría, "Overview of the SMS design method applied to imaging optics," Proc. SPIE **7429**, 74290C (2009).
19. D. Michaelis, P. Schreiber, and A. Bräuer, "Cartesian oval representation of freeform optics in illumination systems," Opt. Lett. **36**, 918–920 (2011).
20. D. Michaelis, P. Schreiber, C. Li, and A. Bräuer, "Construction of freeforms in illumination systems via generalized Cartesian oval representation," Proc. SPIE **8124**, 812403 (2011).
21. Y. Chen, "Thermal forming process for precision freeform optical mirrors and micro glass optics," Ph.D. dissertation (The Ohio State University, 2010).
22. V. I. Oliker, "Mathematical aspects of design of beam shaping surfaces in geometrical optics," in *Trends in Nonlinear Analysis* (Springer, 2002), pp. 191–222.
23. V. I. Oliker, "Freeform optical systems with prescribed irradiance properties in near field," Proc. SPIE **6342**, 634211 (2006).
24. J. H. Mathews and K. D. Fink, "Numerical optimization," in *Numerical Methods Using MATLAB*, 4th ed. (Prentice Hall, 2004), pp. 376–388.
25. Z. F. Zhuang and F. H. Yu, "A contour calculation method for rapid freeform reflector construction with ellipsoid patches," Opt. Laser Technol. **56**, 430–435 (2014).